AAEC/E280

# AUSTRALIAN ATOMIC ENERGY COMMISSION
## RESEARCH ESTABLISHMENT
## LUCAS HEIGHTS

### SOME X-RAY AND NEUTRON MEASUREMENTS ON THE DENSE PLASMA FOCUS

by

G.R. HOGG
J. TENDYS

August 1973

ISBN 0 642 99596 6

AUSTRALIAN ATOMIC ENERGY COMMISSION

RESEARCH ESTABLISHMENT

LUCAS HEIGHTS

# SOME X-RAY AND NEUTRON MEASUREMENTS ON THE DENSE PLASMA FOCUS

by

G.R. Hogg

and

J. Tendys

## ABSTRACT

Measurements of the X-ray and neutron emissions from a dense plasma focus device are given which include time integrated X-ray photographs of the focus, time dependent X-ray and neutron output characteristics and average neutron energy measurements determined by time of flight. The time of emission of X-rays and neutrons has been correlated with the time differential of the plasma current and the results of Bernstein et al. (1969) confirmed. When the focus was operated with a negative centre electrode, the X-ray and neutron emission was ≃ 0.25% of that obtained under identical conditions with a positive centre electrode.

National Library of Australia card number and ISBN 0 642 99596 6

The following descriptors have been selected from the INIS Thesaurus to describe the subject content of this report for information retrieval purposes. For further details please refer to IAEA–INIS–12 (INIS: Manual for Indexing) and IAEA–INIS–13 (INIS: Thesaurus) published in Vienna by the International Atomic Energy Agency.

CATHODES; DATA; DEUTERIUM; ELECTRONS; EMISSION; HYDROGEN; NEUTRONS; PLASMA; PLASMA DENSITY; PLASMA FOCUS; PULSES; TIME DEPENDENCE; TIME-OF-FLIGHT METHOD; X RADIATION; X-RAY SPECTRA

CONTENTS

| | | Page |
|---|---|---|
| 1. | INTRODUCTION | 1 |
| 2. | EXPERIMENT | 1 |
| 3. | X-RAY MEASUREMENTS | 2 |
| 4. | NEUTRON MEASUREMENTS | 4 |
| 5. | NEGATIVE INNER ELECTRODE OPERATION | 4 |
| 6. | CONCLUSIONS | 5 |
| 7. | REFERENCES | 5 |

FIGURE 1 Pinhole camera photographs of the time integrated X-ray emission from the dense plasma focus.

FIGURE 2 X-ray and neutron pulses derived from various filter-detector combinations.

FIGURE 3 Time of flight data for three separate shots at 18 kV and 0.40 kPa (3.0 torr) deuterium.

## 1. INTRODUCTION

The dense plasma focus has been the subject of much investigation (Mather 1965, Bernstein et al. 1969, Maisonnier 1973) and considerable difficulty has been experienced in attempting to correlate the experimental results with theoretical models of the plasma focus. In particular, the mechanism of neutron production within the plasma focus is not understood. Furthermore, there is considerable disagreement on the estimation of electron temperature derived from plasma X-ray measurements.

The present paper is confined to descriptions of the measurements of the X-ray and neutron emission from the dense plasma focus. The measurements are preliminary but necessary as they determine the intensity and spectrum ranges of the X-rays and neutrons emitted. The device was also operated with a negative inner electrode and the results do not agree with those previously reported, although the latter are not very detailed.

## 2. EXPERIMENT

The plasma focus device is of standard construction (Mather 1965). The inner and outer electrodes are respectively of 50 mm and 100 mm diameter and are 200 mm long. A Pyrex glass sleeve extends over the inner electrode for a distance of 50 mm from the breech end. The electrode material is copper and the outer electrode is perforated. The inner electrode has a tungsten insert at the end to reduce erosion which is particularly severe with positive inner electrode operation.

In the work described here the device was normally operated with a positive inner electrode, but the polarity could be reversed. The capacitor bank was operated in the range 18-21 kV corresponding to a stored energy of 13-18 kJ. The gas filling was either hydrogen or deuterium in the pressure range 0.25-1.0 kPa (2-8 torr).

Preliminary X-ray measurements were obtained with a pinhole camera set to view the focus at $90^{\circ}$ to the axis. The pinhole diameter was 1 mm and was covered with 13 μm thick aluminium foil. Kodak Radiation Monitor film was re-wrapped in 50 μm thick black polyethylene foil. The camera was interconnected to the vacuum system of the device, so significant X-ray attenuation occurred only in the two foils. If the electron distribution in the plasma is assumed to be thermal, with a temperature of ~ 1 keV, it can be shown that the camera arrangement has a strong sensitivity in the X-ray energy range 1 to 10 keV except for the region of K-edge absorption in aluminium (1.5-2 keV).

Time resolved X-ray measurements were obtained by recording the output from a silicon surface barrier detector mounted in the film plane of the pinhole camera and from plastic scintillator-photomultiplier assemblies. Both detectors had a rise-time response of 14 nsec, limited by the recording oscilloscope. When operated with suitable absorbing materials, X-ray spectral measurements were obtained. Neutron energy measurements were made with plastic scintillator-photomultiplier assemblies arranged in a time-of-flight configuration. The neutron yield was determined by means of a silver activation detector. The current and voltage characteristics were obtained using, respectively, a Rogowski loop and a low inductance resistive divider.

The focus device is an intense source of RF noise (especially at breakdown) and also of strong time-dependent magnetic fields so great care was taken in shielding and earthing the detectors and other devices, which operate at the same time as the discharge. Consequently all signal cables were double screened.

## 3. X-RAY MEASUREMENTS

The X-ray photographs provide a time integrated view of the X-ray emission. Figure 1 shows a series of three X-ray pinhole photographs from different shots with identical initial conditions of bank voltage and gas filling pressure. The pictures vary greatly but the following features can be discerned on all of them:

(i) A very bright region at the anode and a short jet-like feature just in front of the anode.

(ii) A diffuse cloud-like region extending up to 20-30 mm from the anode and usually of larger diameter than the feature in (i). It should be noted that in a print it is very difficult to reproduce the fine structure observable in the original negatives.

The typical time-varying X-ray output consists of two pulses as shown in Figure 2(a). The first pulse is a combination of a soft X-ray pulse of energy less than 15 keV and a hard pulse of $\sim$ 50 nsec width containing X-rays with energies of several hundred keV. This is deduced from the difference of the widths of the first pulse in Figure 2(a) (X-ray energy $\geqslant$ 1 keV) and of the first pulse in Figure 2(b) (X-ray energy $\geqslant$ 15 keV). The energy of the hard X-rays in the first pulse must exceed 200 keV as indicated by the existence of a substantial component in Figure 2(c). Because of the constancy of the shape of this hard pulse as absorber thickness is reduced, the spectral shape of the hard component must be fairly sharp with no substantial part of the distribution below an energy of 100 keV. The soft component of the first X-ray pulse probably originates from the heating of the deuterium plasma during the formation of the focus and the hard component originates from runaway electrons from the plasma in collision with the anode, soon after the collapse of the current front.

The second X-ray pulse shown in Figure 2(a) occurs some 300 nsec after the first pulse and is much broader. The energy of these X-rays is mainly in the range 1-15 keV (this pulse is largely attenuated in Figure 2(b)) and at no stage of the operation of the focus device has any hard (~ 100 keV) component been detected in this pulse, or at any other time after the initial hard pulse. Because of the high intensity of this second pulse, and of its timing with respect to the initial pinch stage, it is most unlikely that it is associated with the deuterium plasma and most likely originates from the high Z ions blown off the end of the electrodes by the intense electron bombardment. Spectral measurements by Bernstein et al. (1969) show the existence of strong CuKα and WLα,β,γ lines at this time.

It is thus determined that the first X-ray pulse corresponds spatially to the bright region at the anode and the short jet-like feature in front of the anode, visible in Figure 1. The later soft X-ray pulse can be identified with the diffuse region surrounding the bright feature (only small parts of this diffuse region are discernible in Figure 1).

The time correlation between the X-ray output and the time rate of change of current in the focus (dI/dt) is shown in Figures 2(a) and 2(e) where only the hard X-ray pulse is shown. The hard X-ray pulse starts within 20 nsec of the maximum compression of the current front (i.e. dI/dt minimum). Figure 2(a) shows that some of the soft components of the first pulse begin at a time earlier than the hard component. The dI/dt pulse shown is double peaked, corresponding to a bounce in the compression wave of the plasma. The dI/dt pulse is generally double peaked, the first peak always being predominant. The fine structure of the dI/dt pulse is not reflected in the neutron pulses and although there are two neutron pulses, only one hard X-ray pulse is observed. The small pulse observed at ~ 300 nsec after the first neutron pulse in Figure 2(c) is, in fact, a second neutron pulse, since no part of it appears at the corresponding time in Figure 2(b).

More detailed spatial and time resolution can be obtained by using a series of surface barrier detectors in the image plane of the pinhole camera. Energy resolution can be obtained by using K-edge and Ross filters. It is possible to obtain the X-ray spectrum in the energy range 1-30 keV by this method with resolution approaching 0.5 keV (Mather et al. 1971). At some expense in time resolution, the spatial resolution for the various energy components can be improved by using filters in front of a scintillator sheet at the pinhole image plane and then observing the visible image produced with an image converter camera.

## 4. NEUTRON MEASUREMENTS

The total neutron output was measured with a silver activation counter placed in a position at $90^{\circ}$ to the axis with an acceptance angle of 2 steradians. The total number is then derived by assuming that neutron emission is isotropic. The number of neutrons per shot was approximately $10^9$, but shot to shot variations of more than a factor of 10 were observed.

The time dependent neutron emission at $0^{\circ}$ was measured with a photomultiplier plastic scintillator assembly shielded with lead to attenuate the hard X-ray pulse. Figure 3 shows the outputs of two detectors set at 1.78 and 10.72 m from the source along the axis. The hard X-ray pulse is marked and the flight time of the neutrons to the more distant detector is observable. The X-ray pulse was used for exact time correlation of the pulses. The peak of the neutron pulse has an average velocity of 23.1 mm/nsec, equivalent to a neutron energy of 2.8 MeV. This value is similar to that obtained by Lee et al. (1971). The three different sets of results indicate the variability of the shape and magnitude of the neutron and X-ray outputs. Further analysis of the time-of-flight data shows that the maximum and minimum energies of the neutron spectrum are at least 3.4 and 1.9 MeV respectively. Nuclear emulsion studies by Bernstein et al. (1969) indicate that these are the limits of the spectrum in the $0^{\circ}$ direction.

The time of formation of the neutron pulse is obtained by correcting for the neutron time of flight. For Figures 2(b) and 2(c) the detectors were 1.46 m from the source which corresponded to a flight time of 63 nsec at an average neutron energy of 2.8 MeV, (or 60 nsec for peak energy of 3.1 MeV). This places the start of the neutron pulse in coincidence with the start of the hard X-ray pulse (with an experimental error of $\pm$ 10 nsec). Furthermore, the start of the neutron pulse occurs at the peak of plasma compression (corresponding to a minimum in the dI/dt trace). This fact is important for the model of neutron production proposed by Bernstein et al. (1969). Patou et al. (1968) also found that about 1 per cent of the neutron emission is contained in a low level emission just before the main pulse. This is rather difficult to detect and while no real evidence exists for it in our results, it is not inconsistent with them.

## 5. NEGATIVE INNER ELECTRODE OPERATION

The results obtained with positive inner electrode operation are generally satisfactory, except for the non-repeatibility of shots, a factor that seems to be inherent in the device itself. The literature (Mather 1966, Butler et al. 1969, Maisonnier 1973) indicates that the polarity of the inner electrode is not a factor affecting the operation of the device except for a reduced neutron yield. With pure deuterium gas filling it was observed over a series of shots that for a negative inner electrode the neutron yield was reduced by a factor of 1/400 over that obtained under identical conditions with a positive inner electrode. The X-ray yield was also severely reduced which is to be expected from the decelerating effect of the negative inner electrode on electrons from the plasma. Furthermore, a strong focus, as indicated by the magnitude of the dI/dt wave, was only rarely obtained and even a weak focus was obtained only about 20 per cent of the time. Image converter camera photographs indicated an increased tendency for electrical breakdown across the insulator shortly after the front of the current sheath had passed the end of the insulator and before the sheath had collapsed off the end of the electrodes. This breakdown, which was also observed for low pressure [~0.13 kPa (1 torr) $D_2$] positive inner electrode operation, effectively short circuits the electrodes and prevents the stored energy of the capacitor bank being transferred to the plasma.

## 6. CONCLUSIONS

Preliminary measurements of the X-ray and neutron emissions have been made to give data for the future setting up of detailed measurements. Some information on the parameters of our plasma focus was obtained at the same time. The X-ray and neutron burst shapes, their variability from shot to shot and the crude spectral data obtained are all consistent with measurements made by other workers on similar machines. The time correlation between the X-ray and neutron outputs and the dI/dt characteristics have been determined and the results of Bernstein et al. (1969) confirmed.

Operation of the dense plasma focus with a negative centre electrode was not consistent with previously reported data. The neutron emission was usually about 0.25 per cent of the emission for similar conditions with a positive centre electrode. The X-ray output was also considerably reduced. The tendency for the increased probability of breakdown across the glass insulator is not presently explainable.

## 7. REFERENCES

Bernstein, M.J., Meskan, D.A. and Van Paassen, H.L.L. (1969) - Phys. Fluids 12 (10) 2193.

Bernstein, M.J., Lee, C.M. and Hai, F. (1971) - Phys. Rev. Lett. 27 : 844.

Butler, T.D., Henins, I., Jahoda, F.C., Marshall, J. and Morse, R.L. (1969) - Phys. Fluids 12 (9) 1904.

Lee, J.H., Shomo, L.P., Williams, M.D. and Hermansdorfer, H. (1971) - Phys. Fluids 14 (10) 2217.

Maisonnier, C. (1973) - Proc. 5th European Conf. on Controlled Fusion and Plasma Physics, August 1972, Grenoble, France (in Press).

Mather, J.W. (1965) - Phys. Fluids, 8 (2) 366.

Mather, J.W. (1966) - Proc. 2nd Conf. on Plasma Physics and Controlled Nuclear Fusion Research, 6-10 September 1965, Culham, Berks, England STI/PUB/111, Vol.II p389. IAEA, Vienna.

Mather, J.W., Bottoms, P.J., Carpenter, J.P., Ware, K.D. and Williams, A.H. (1971) - Proc. 4th Conf. on Plasma Physics and Controlled Nuclear Fusion Research, June 17-23, 1971, Uni of Wisconsin pp 561-570. IAEA Vienna.

Patou, C., Simonnet, A. and Watteau, J.P. (1968) - J. de Phys. 29 : 973.

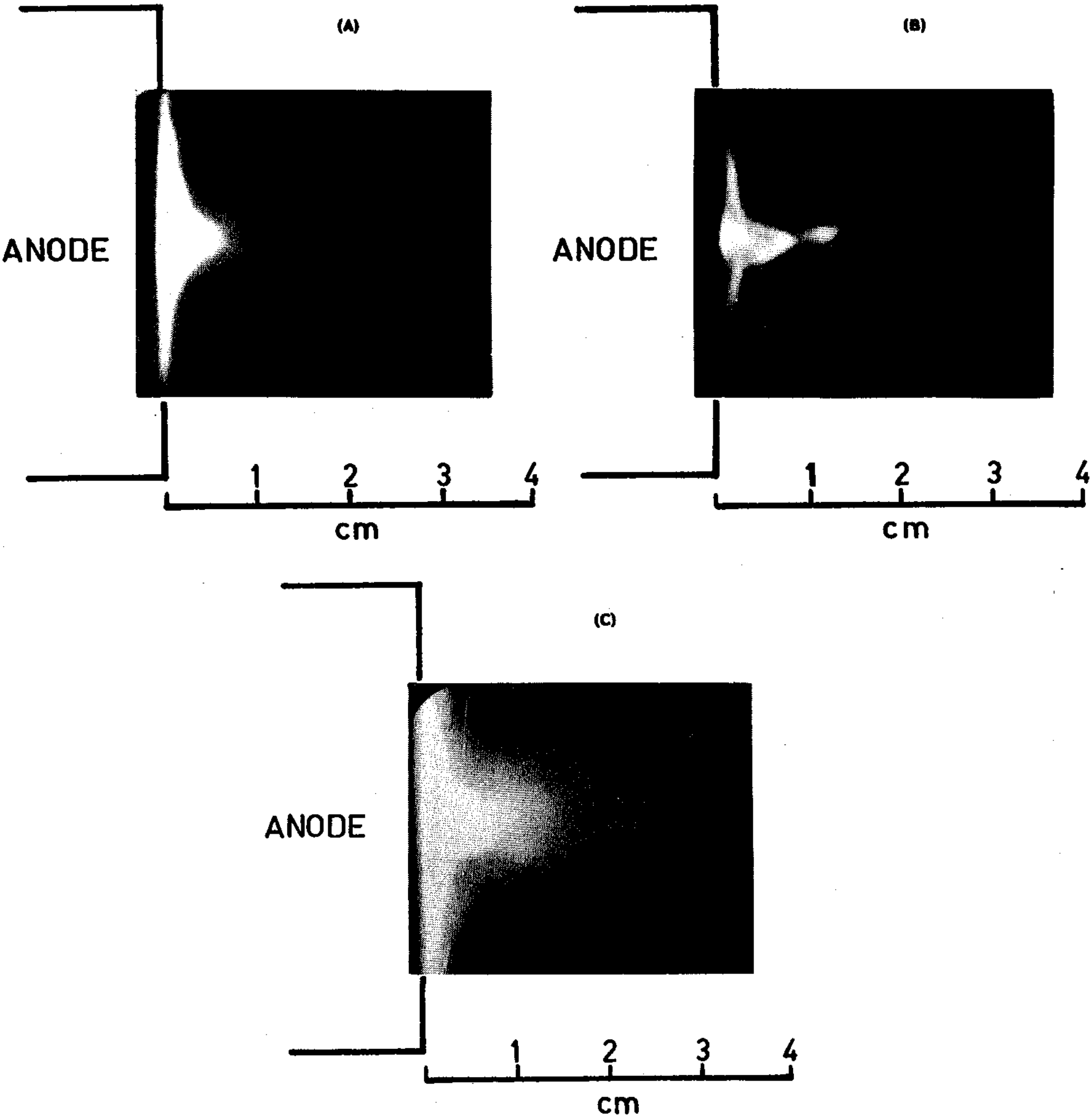


**FIGURE 1. PINHOLE CAMERA PHOTOGRAPHS OF THE TIME INTEGRATED X-RAY EMISSION FROM THE DENSE PLASMA FOCUS**

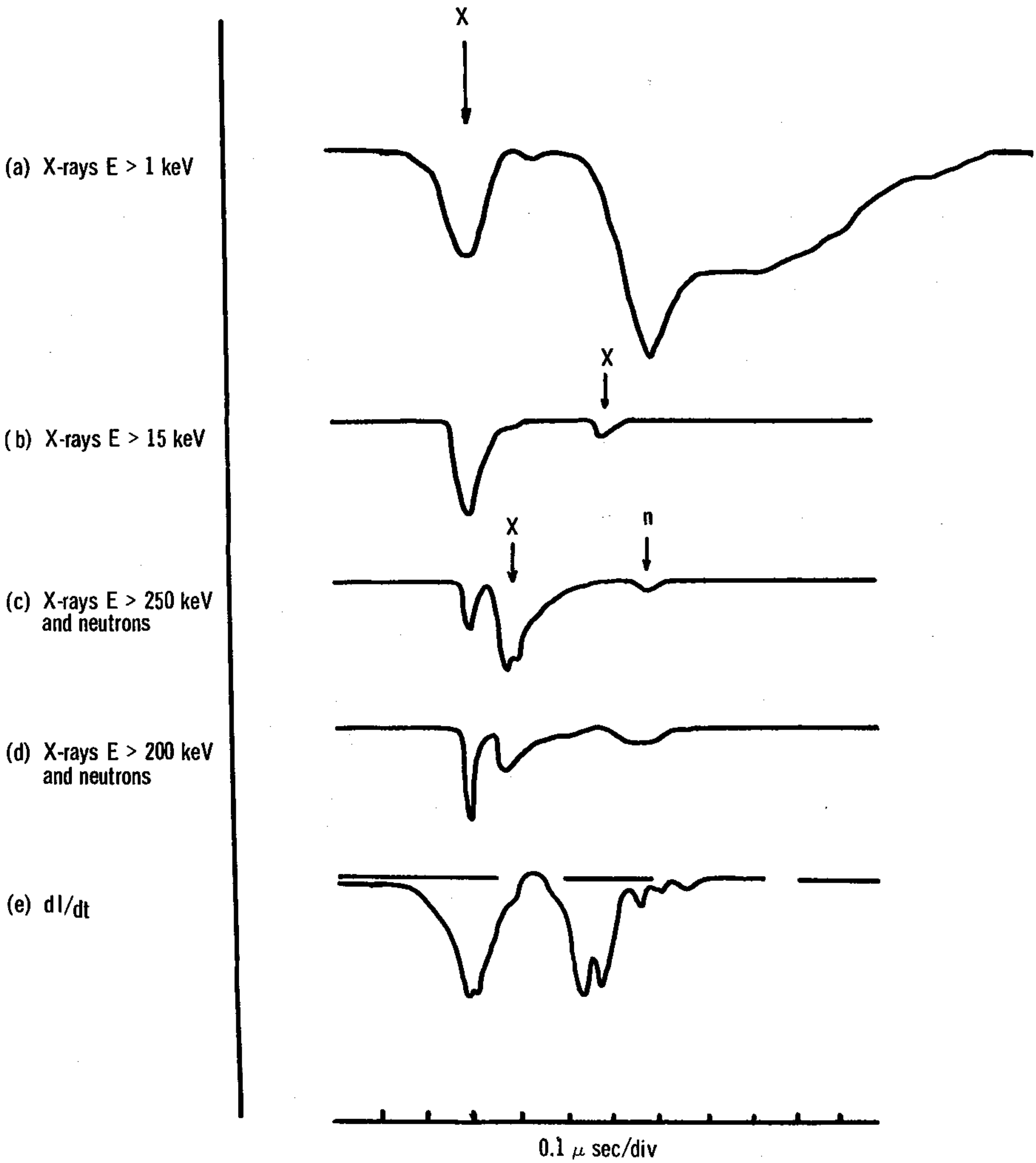


**FIGURE 2. X-RAY AND NEUTRON PULSES DERIVED FROM VARIOUS FILTER-DETECTOR COMBINATIONS**

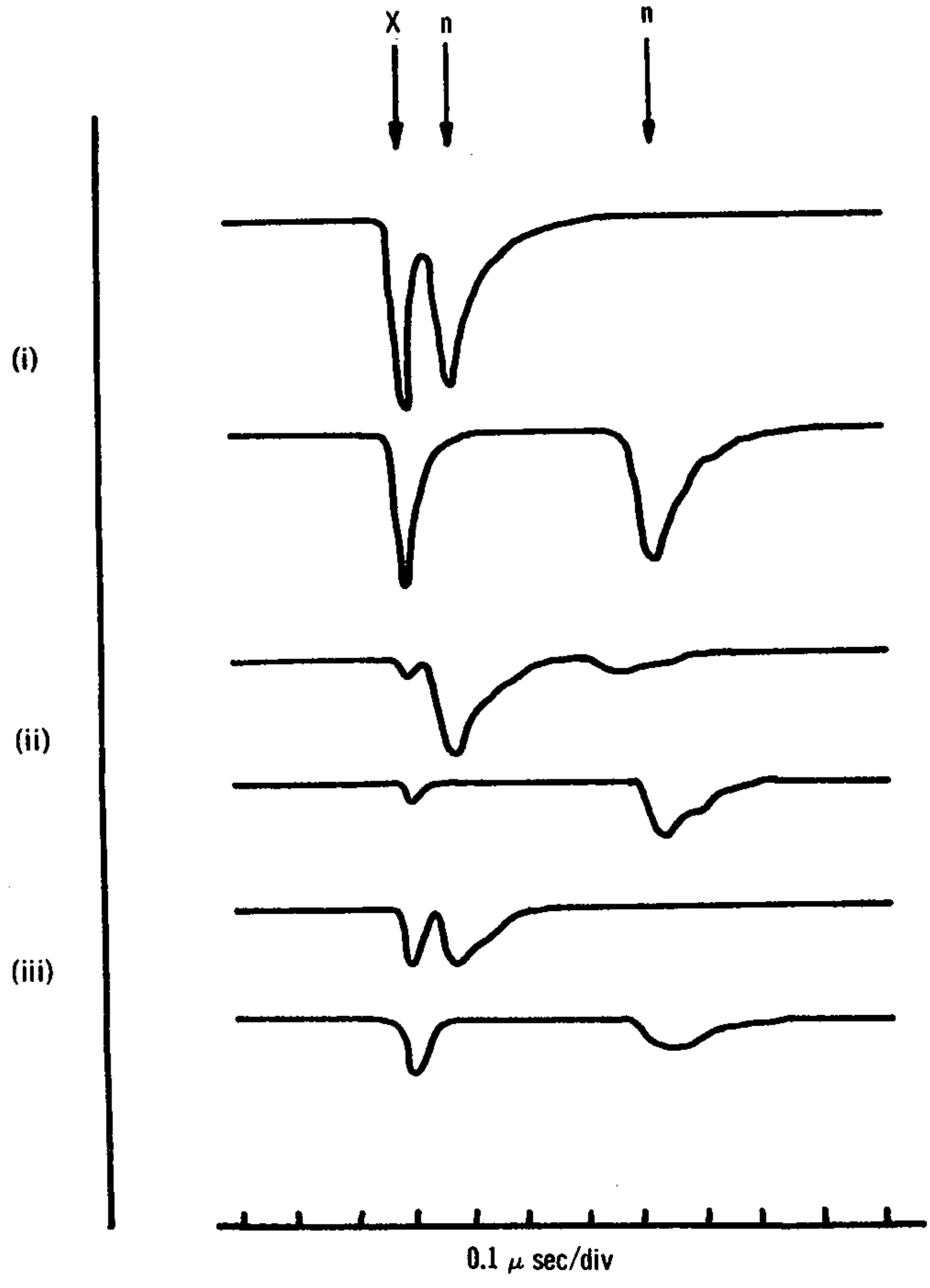


FIGURE 3. TIME OF FLIGHT DATA FOR THREE SEPARATE SHOTS AT 18 kV AND 0.40 kPa (3.0 torr) DEUTERIUM